Interfacial and Mechanical Property Comparison of Cu/Al Composite Plates Manufactured by Rolling and Underwater Explosive Welding

Dapeng Zhou[1, 2], Zhongshu Liu[3, 4], Jiawen Huang[3, 4*], Jinhua Chen[1, 2*], Xiang Chen[3, 4*], Xiaohong Zhou[1, 2]

[1] CCTEG Huaibei Blasting Technology Research Institute Co., Ltd., Anhui 235099, China; [2] Anhui Key Laboratory of Explosive Energy Utilization and Control, Anhui 235099, China; [3] State Key Laboratory of Precision Blasting, Jianghan University, Wuhan 430056, China; [4] Hubei Province Key Laboratory of Engineering Blasting, Jianghan University, Wuhan 430056, China

Abstract: Cu/Al composites are widely utilized across various industries due to their lightweight and excellent electrical conductivity. However, the impact of different manufacturing methods on the interfacial structure and mechanical properties of these composites remains significant. In this study, Cu/Al composite plates were fabricated using rolling and underwater explosive welding techniques to systematically compare their interfacial microstructure and mechanical performance. Interface morphology, grain orientation, grain boundary characteristics, and phase distribution were analyzed through optical microscopy, scanning electron microscopy, and electron backscatter diffraction. Mechanical properties were assessed using tensile shear tests, 90° bending tests, and hardness measurements, with Vickers hardness and nanoindentation tests providing further insight into hardness distributions. The results indicate that the diffusion layer in rolled Cu/Al composites is relatively fragile, while those produced by underwater explosive welding feature a diffusion layer approximately 18 μm thick, metallurgically bonded through atomic diffusion. The tensile shear strength of these composites ranges from 64.14 to 70.84 MPa, with superior flexural performance demonstrated in the 90° three-point bending test by the underwater explosive welded samples. This study elucidates the effects of distinct manufacturing methods on the interfacial properties and mechanical performance of Cu/Al composites, offering essential insights for selection of manufacturing method and application.

Key words: underwater explosive welding; Cu/Al composites; rolling; EBSD; nanoindentation

With the continuous development of manufacturing technology, Cu/Al composites have received widespread attention due to their lightweight nature, electrical conductivity, thermal conductivity, and corrosion resistance. They have a wide range of applications, particularly in the automotive [1-3], aerospace [4], and marine fields [5,6]. Copper has a density three times that of aluminum, and its melting temperature is approximately 60% lower than that of copper . Therefore, using Cu/Al composites instead of pure copper can significantly reduce total cost and quality while improving practicality. However, achieving reliable Cu/Al bonding presents challenges, as the differences in physical properties, such as density, melting

temperature, and thermal expansion, can result in stress and structural inconsistencies at the interface. Effective bonding requires techniques to manage these disparities, enhancing joint quality and durability. Currently, most Cu/Al composites are fabricated using stirring friction [7], rolling, electropulsing [8-9], laser welding [10] and explosive welding [11-14]. These diverse production methods create diverse interface distributions. Payak et al.[15] for Cu/Al concentrated on various parameters of stir friction and the defects that develop, emphasizing the role of interlayers in stir friction Cu/Al composites. Barekatain et al.[16] used a typical dynamic shoulder welding technique to fuse AA1050 and pure Cu, and discovered that the material was significantly mixed in the stirring zone, with most joints containing a combination of Al and Cu positions, as well as voids and cracks. Lin et al. [17] determined that the grain size and thickness of the diffusion layer are the primary factors influencing the mechanical characteristics of Al/Cu laminated composites. Chang et al. [18] performed numerical simulations of rolled bonded Cu/Al and discovered that the interfacial layer formed in four stages: copper-aluminum surface contact, contact surface activation, mutual diffusion of copper-aluminium atoms, and reaction diffusion. Sas-Boca et al. [19] attempted to analyze the bonding of an Al-Cu bimetallic composite layer via hot rolling, but the bonding was inadequate, and the presence of some oxides inhibited bonding, resulting in fissures. Wei et al. [20] used explosion welding, cold pressure welding, and solid-liquid casting to create Cu/Al composites and determined that explosive welding is the most advantageous approach. Jiang et al. [21] investigated the influence of stand-off on the thickness of a localised molten layer in explosively welded Cu/Al.

Rolling over the interface at the solid solution and mechanical occlusion in the thickness direction produces high compressive stress, which binds the metal composite together. Its main problem lies in the incomplete metallurgy due to insufficient diffusion layer. Explosive welding involves the use of explosives to cause two or more layers of the same or dissimilar metals to collide obliquely at the interface, resulting in local high temperature, high pressure, and substantial plastic deformation, thereby welding the metals together [22-24]. The control of the thickness of the melted layer in Cu/Al explosive composites is crucial. Moreover, for thin metal plates [25], it is essential to avoid excessive melting of the interface, breaking of the parent material, and other impacts on the quality of the combination. Underwater explosive welding [26] is advantageous in this regard; the explosive welding composite device is placed underwater, and water is used to replace air as the propagation medium of the blast energy. This reduces contact with oxygen and allows the completion of the composite metal plate, which cannot be achieved in air. Underwater explosive welding has indicated advantages in composite thin materials, brittle, and hard materials, and difficult-to-process materials throughout extensive studies [27-30].

In this study, Cu/Al composite samples were prepared utilizing rolling and underwater explosive welding respectively, with an emphasis on analyzing the interfacial microstructure and mechanical properties and comparing the interfacial characteristics of various composite processes. The morphological properties of the interface, and the grain orientation, grain boundary features, and phase distribution of the materials were investigated using an optical microscope (OM), a scanning electron microscope (SEM), and electron backscattering diffraction (EBSD). Tensile shear, 90° bending, and hardness tests were utilized to assess mechanical qualities, with Vickers hardness and nanoindentation tests employed to thoroughly analyze the samples' hardness characteristics. The findings will help to better understand the preparation process, interfacial characteristics, and mechanical properties of Cu/Al composites, serving as a valuable reference for optimizing the preparation process and enhancing material qualities.

1 Experimental procedure

1.1 Experimental materials and methods

This study used two composite methods: rolling and explosive welding. The materials used for rolling and explosive welding are identical, with specific parameters outlined in Table 1. Notably, the surface density of T2 copper is 8.92 g·cm^{-3}, while the density of A1060 aluminum is 2.71 g·cm^{-3}, indicating a significant difference in their physical properties. The rolled Cu/Al composite plates are commercially available transition plates sourced from LUOYANG COPPER (GROUP) CO., LTD. A schematic diagram of the underwater explosive welding apparatus for the Cu/Al composite plates is presented in Fig. 1. To enable effective energy transfer in the water tank, a 15 mm thick explosive layer with a density of 1.2 g·cm^{-3} and an explosion velocity of 3500 m·s^{-1} was affixed beneath a supporting bracket, positioned at a distance of 15 mm from the flyer plate. The stand-off distance between the flyer plate and the base plate was maintained at 0.2 mm. Prior to welding, the contact surfaces of the Cu and Al plates were prepared through sanding and polishing to improve surface finish and flatness, enhancing contact performance and welding quality.

Table 1 Process parameters

Sample	Materials	Process	Medium
1	T2 copper (0.5 mm) + A1060 (4.5 mm)	Rolling	Air
2	T2 copper (2 mm) + A1060 (8 mm)	Explosive welding	Water
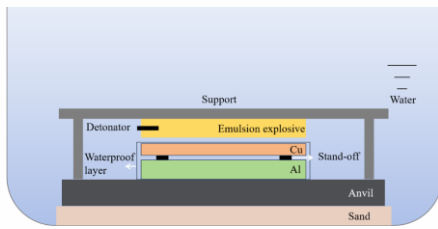
Fig. 1 Schematic diagram of an underwater explosive welding device.

1.2 Microstructure analysis and mechanical property analysis

Microstructure and mechanical property examination of experimental samples involved an in-depth investigation and analysis of the samples' microstructure and properties from multiple dimensions and angles. Initially, the specimens were cut by wire-cut and then processed metallographically with resin inlay. The two-dimensional microscopic morphology of the samples was examined using an OM (ZEISS Axiolab5) and an SEM (ZEISS Sigma 300) to gain insight into the microstructural and morphological properties of the sample surfaces. The OM provided high-resolution images to observe the external morphology and surface details of the samples. Additionally, the SEM provided higher magnification and more detailed surface information, revealing more details of the sample's microstructure. Electron dispersive spectroscopy was a widely used technique for elemental analysis. It could detect the distribution of different elements in the samples and comprehend the content and distribution status of various elements in the sample, thereby providing a reference basis for future analysis. Furthermore, EBSD scanning electron microscopy (QUANTA FEG 450 edax) with Orientation Imaging Microscopy (OIM) analysis (version 6.2) software was used to study the grain orientation, grain boundary characteristics, and phase distribution of the samples with a step size of 0.3 μm. This analysis revealed vital information, such as the crystal structure of the material and the direction of grain growth, providing robust support for understanding and optimizing the material.

Second, mechanical property tests were conducted, including tensile shear, 90° three-point bending, and hardness tests, to thoroughly analyze the samples' mechanical characteristics and changes. The tensile shear test evaluated the composite samples' interfacial shear condition and strength. Contrarily, the 90° three-point bending test evaluated the material's flexural performance, deformation behavior under bending load, and bending strength. Vickers hardness and nanoindentation tests were performed to completely examine the hardness characteristics of samples. The Vickers hardness test reflected the material's hardness at the macroscopic level, providing an overall hardness evaluation. Meanwhile, the nanoindentation test allowed for in-depth observation and analysis of the material's mi-

croscopic hardness changes, revealing the hardness of the material's weld interface and other subtle characteristics.

2 Results and Discussion

2.1 OM and SEM results

The composite structure was evaluated through OM and SEM. Rolling was aided by solid solution and mechanical occlusion at the interface, resulting in a relatively thin diffusion layer. The presence of the diffusion layer in rolling was nearly imperceptible under an OM, and the interface appeared smooth and straight. And explosive welding composite is created by applying high energy from the explosion to the flyer plate collision base plate, resulting in rapid composite formation. Under an OM, the oblique collision causes the bonding interface of explosive welding samples to form a micro-wave-like shape, and the wave-like interface enhances the contact area of Cu and Al while also improving the mechanical locking strength of the interface.The impact of the flyer plate on the base plate converts its kinetic energy into thermal energy, resulting in a strong plastic flow of metal and a localized melting layer up to 30 μm.

The SEM revealed a diffusion layer in the rolled sample (Figs. 3b-c). Cu element diffusion was measured at approximately 1 μm inline scanning, while Al element diffusion was measured at approximately 2 μm, indicating a significant diffusion of Al compared to Cu. Vertical cracks perpendicular to the direction of explosive welding were detected in the molten layer of the underwater explosive welded samples, caused by thermal strains generated at the interface during rapid solidification at high temperatures [31]. Cracks in the molten layer of explosive welds were a common event [32,33], and they tend to form in the thicker part of the molten layer without propagating into the base material. According to the mapping scan results, the melting layer primarily consisted of Al, with Al components also diffused on the Cu side. Line scan findings indicated Cu element diffusion of approximately 18 μm and Al element diffusion of approximately 16 μm. The higher diffusion of Al elements compared to Cu elements within the melted layer suggested a significant diffusion capacity for Al. Numerical simulations in Li's study [34] revealed the temperature dependence of interfacial diffusion between the Al and Cu. The interface temperature in the explosive welding method could exceed 1,500 K [35], as indicated by numerical explosively welded samples was substantially more extensive than that of the rolled samples. The presence of a certain diffusion layer can effectively enhance the bond strength of the interface [36,37]. The diffusion capacity of Al elements is greater than that of Cu, both in rolling and in underwater explosive welding.

Rolling   Explosive welding
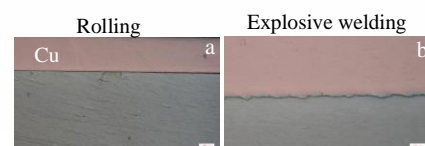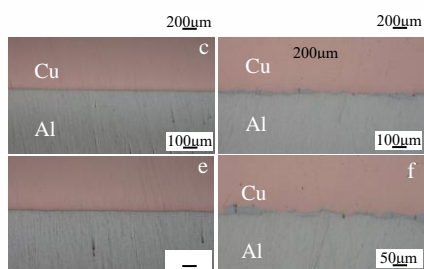
Fig. 2 Optical microscope results: (a, c, and e) rolling; (b, d, and f) explosive welding.
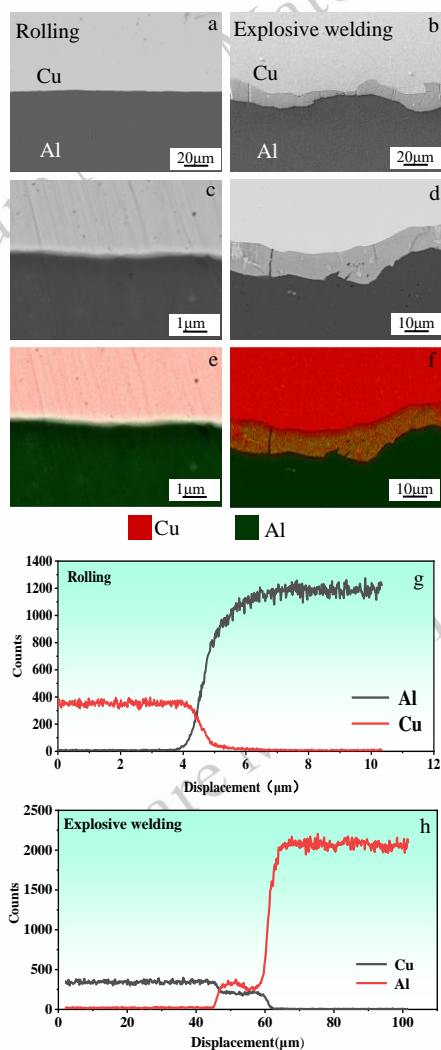
Fig. 3 SEM-BSE results of the interface: (a–c) sample 1; (d–f) sample 2; (g) line scan of sample 1; (h) line scan of sample 2.

2.2 EBSD analysis results

Grain and structural studies were conducted using EBSD to gain a better understanding of grain size, grain boundary changes, phases, interfacial stress distribution, and recrystallization of the samples, comparing interfacial distributions under different conditions. The Kernel average misorientation (KAM) plots in Fig. 4e-f show that rolling composite samples had lower KAM values than explosive welding samples. It is

well understood that the KAM value can reflect the degree of variation in local orientation inside a grain, suggesting that the higher the KAM value, the greater the orientation variance within the grain, which is typically linked with more plastic deformation or dislocation density. Although the rolling process can produce persistent compressive stress and plastic deformation, the explosive welding shock wave can produce greater transient compressive stress and local plastic deformation, resulting in more intense compression and plastic deformation in explosive composite samples. In contrast, the lower nuclear mean orientation of the melted layer in explosive welding (Fig. 4f) indicates that large pressure and plastic deformation occurred on both sides of the interface, and that the nuclear mean orientation was greater on the Al side than on the Cu side, owing to the high strain caused by the greater compressive stress and plastic deformation on the Al side[38,39]. Enrichment of large-angle grain boundaries at the explosive welding interface (Fig. 4b) did not occur in the rolled samples. The increase in large-angle grain boundaries indicates a rise in crystal energy and an increase in recrystallisation fraction. In Fig. 4d, this statement is verified by the large number of fully recrystallised grains distributed at the explosive welding interface, implying that it has a uniform strain distribution. The Cu side of explosive welding has largely recrystallized grains, while the Al side experiences strong plastic deformation about 10 μm away from the contact, resulting in deformed grains. Comparing Cu to Al, low stacking fault energy materials are available[40, 41]. Cu is prone to dynamic recrystallization and the development of equiaxed fine crystals near the explosive welding interface due to the high temperature effect, as a result of the wide extended dislocations that make dislocation climbing unfavorable; Conversely, Al, being the side with the highest stacking fault energy(SFE), is more vulnerable to deformed grains and dynamic restitution because of the restricted width of the extended dislocations, which can climb and cross-slip.

Fig. 5 depicts the grain distribution between Cu and Cu-Al complexes. Grain refinement occurred along the interface in both rolled and explosively welded samples. The grain refinement observed in the explosive welding samples was more extreme. After being heated at high temperatures by explosive welding, the atoms' diffusion ability increases, and the grains form fine isometric crystals via re-nucleation. The grain size of the rolled samples was significantly larger than that of the explosion welded samples, which was due to a difference in the base material as well as grain refinement caused by the increased compressive stress and plastic deformation produced by explosive welding. The grain size statistics were performed on the equivalent circular diameter of the grains. The average grain size in rolling samples was 5.65 μm for Cu, 0.65 μm for Cu-Al, and 2.11 μm for Al, whereas in explosive welding samples it was 0.95 μm for Cu, 0.94 μm for Cu-Al, and 2.25 μm for Al. Ultrafine grain (UFG) is defined as a grain size of

less than 1 μm and has been shown to improve mechanical qualities like tensile strength [42] and creep behavior [43].

Fig. 6 depicts the texture distribution of Cu/Al composite plates, which aids in further analyzing its preferred direction. The Cu/Al composite plates interface has five types of textures: deformation textures (S texture {123} < 634 >, Copper texture {112} < 111 >, and Brass texture {011} < 112 >), and recrystallization textures (Goss texture {011} < 100 >, Cube texture {001} < 100 >). In the rolling samples, the S and Cube textures are largely spread on the Cu side, whereas the Brass texture is predominantly distributed on the Al side. In explosive welding samples, on the other hand, texture irregularity is always seen along the interface, with the recrystallization texture Goss texture and Brass texture having the greatest overall

dispersion. Compared to the recrystallization distribution map in Fig. 4c, the Goss texture was distributed on the recrystallized grains, while the Brass texture was scattered on the deformed grains. Deformation texture generally causes material anisotropy, which is detrimental to mechanical stability[44]. The rolled samples showed a higher deformation texture. Analysing the polar plots of the samples, both in the rolled and in the explosive welding samples, the strength of the weave on the Al side (Rolling,max= 10.9; Explosive welding, max= 9.84) is higher than that on the Cu side (Rolling,max= 6.51; Explosive welding, max= 3.26). Dynamic recrystallization limits weave transformation[45], weakening the texture, whereas the Cu side was more prone to dynamic recrystallization, resulting in a low-intensity texture.
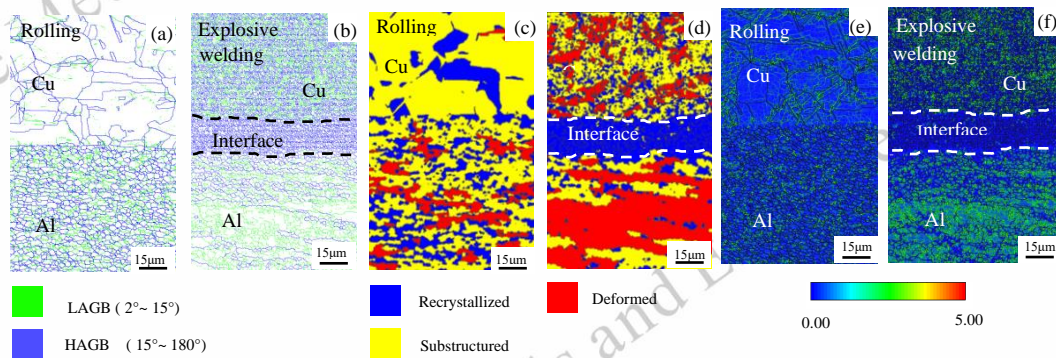
Fig. 4 EBSD results of Cu/Al composite plates interface: (a-b) grain boundary map; (c-d) recrystallization distribution map; (e-f) KAM map.
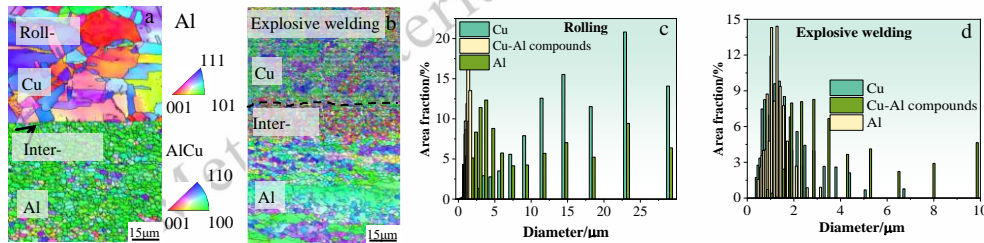
Fig. 5 Grain distribution at the interface of Cu/Al composite plates: (a-b) IPF map; (c-d) grain size map.
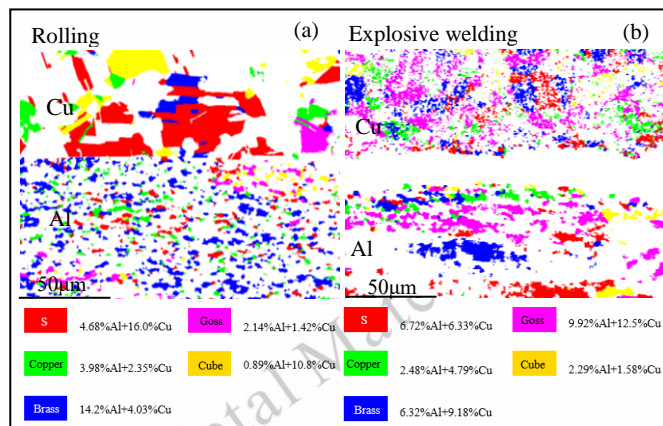
Fig. 6 Interfacial texture distribution of Cu/Al composite plates.

407
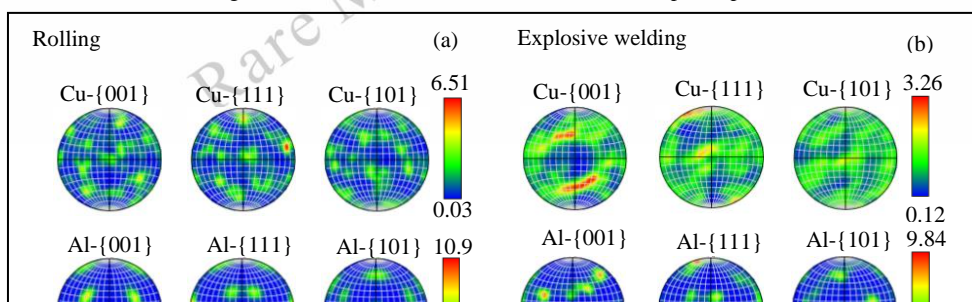
2.3. Mechanical property analysis

Mechanical testing results further substantiate the impact of processing techniques. The tensile shear test was used to evaluate the interfacial shear strength of the composite, reflecting the bond strength at the interface. Only the underwater explosive welding samples (Fig. 8a) were studied because the upper layer of the rolled samples was excessively thin (0.5 mm), which made sampling difficult. All samples were fractured at the weld contact, with shear strengths ranging from 64.14 to 70.84 MPa, indicating consistent findings. The sample fracture did not exhibit a plateau phase, as observed in the curve graph, indicating a brittle fracture. Cu and Al are both FCC crystal structures, and in general the FCC crystal structure usually remains in a ductile fracture mode, but after being subjected to cold working by explosive welding which increases the dislocation density, the fracture mode is converted from ductile fracture to brittle fracture. The fracture after tensile shear was analyzed using XRD, and only Cu elements were detected on the Cu side, while Al elements and the compound $AlCu_3$ were detected on the Al side. This implies that the fracture occurred at the interface between Cu and the melted layer, where the melted layer contained $AlCu_3$ and Al elements.

The bending performance of the samples was evaluated by performing 90° bending experiments, and no significant delamination or cracking was observed in either group of samples, which successfully withstood 90° bending from both the Cu and Al sides. However, the measured bending strength of the explosive welding samples (227.64~343.18 MPa) was significantly better than that of the rolled (234.85~257.17 MPa).

The state of interfacial deformation influences the hardness. The hardness of the samples was analyzed using Vickers hardness and nanoindentation hardness tests, and it was discovered that the hardness variance between rolling and underwater explosive welding samples was significantly different. Vickers hardness was measured with a test force of 0.2 kg. The hardness of the underwater explosive welding samples increased as they approached the contact on the Cu side and decreased as they approached the interface on the Al side.
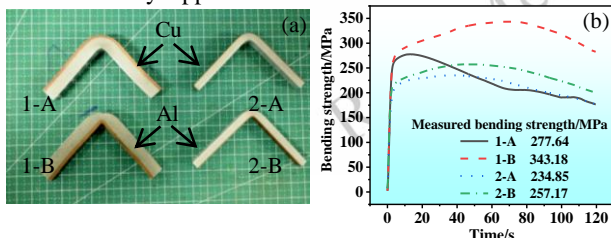
Contrarily, the rolling samples had the opposite tendency. Grain refinement also occurred in the rolled samples on the Al side near the interface in grain Fig. 5 in the EBSD assay, and grain refinement contributes significantly to hardness strengthening[46]. Work hardening and grain refining also contributed to increased hardness at the Cu side of the underwater explosive welding samples at the contact. However, strain softening occurred on the Al side during EBSD testing due to high SFE and dynamic recovery during explosive welding, counteracting work hardening. Therefore, the closer to the interface, the harder the Al side became. To examine the hardness of the melted layer in explosive welding samples, nanoindentation experiments were performed with a test force of 1000 μN. Each point was indented at 5 μm intervals, totaling 30 spots for reference. Near the interface, both rolling and explosive welding indicated a slight increase in hardness, consistent with the grain refinement observed in the IPF of EBSD. The melted layer exhibited much higher hardness than the parent material, with a maximum nano-hardness of 16.44 Gpa, attributed to the presence of intermetallic compounds and grain refinement. These metal compounds tend to behave hard and brittle. Simultaneously, Cu particles entered the melting layer, while hardness remained unaffected near the fissures.

Fig. 8 Results of tensile shear sample; (b) tensile shear curve; (d) X
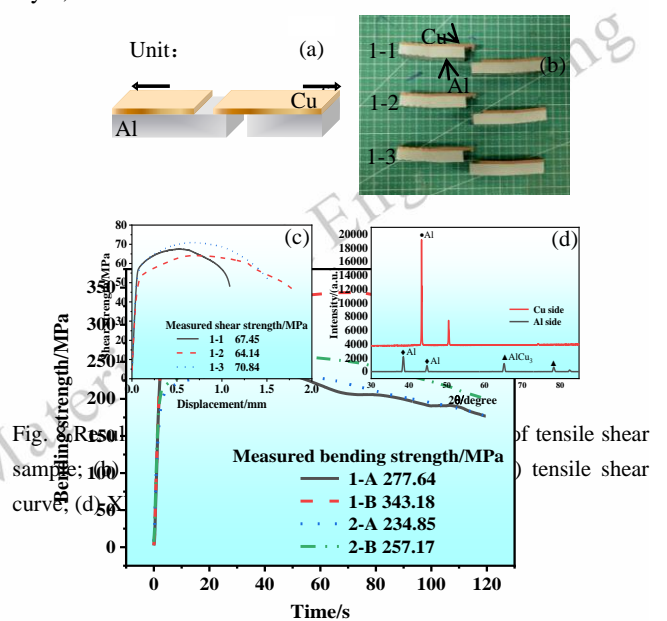
Fig. 9 Results of 90° bending test: (a) 90° bending test diagram of the

samples; (b) 90° bending test curve.
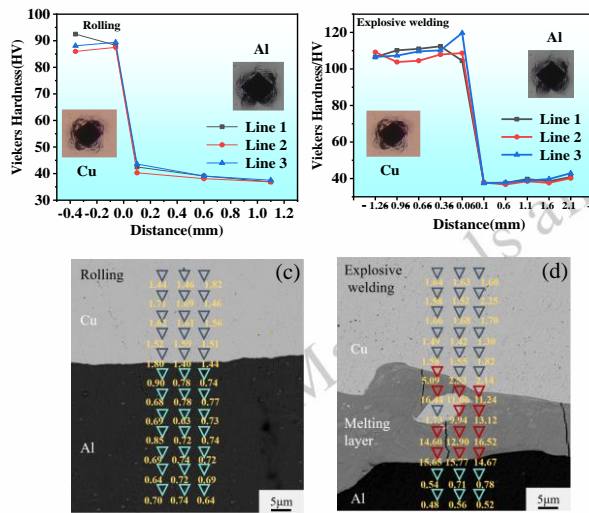
Fig. 10 Results of hardness: (a) Vickers hardness of sample 1; (b) Vickers hardness of sample 2; (c) Nano-hardness of sample 1;(d) Nano-hardness of sample 2.

3 Conclusions

1) The rolling-produced samples were compounded at the interface by solid solution and mechanical occlusion; the interface was straight and flat, with a thin diffusion layer about 2 μm thick. The underwater explosive welding samples exhibited a microwave-like interface with a diffusion layer of approximately 18 μm, including AlCu3 and Al elements. The diffusion capacity of Al was stronger in both sets of samples compared to Cu. Both explosive welding and rolling produced grain refinement, but the grain refinement was more pronounced in explosive welding, especially in the region near the interface.

2) The high SFE of Al in underwater explosive welding samples caused high strain and strong texture due to increased compressive stress and plastic deformation. The grains were largely distorted on the Al side, while on the Cu side, they were recrystallized. In the rolled samples, the deformation texture S texture was most distributed, while in the underwater explosive welding samples, the recrystallisation texture Goss texture was most distributed, which was more beneficial for the stable mechanical properties.

3) The tensile shear strengths of the underwater explosive welding samples ranged from 64.14~70.84 MPa, with AlCu3 detected at the fracture. Both the underwater explosive welding and rolling samples withstood the 90° bending test, but the explosive welding samples (227.64~343.18 MPa) outperformed the rolling samples (234.85~257.17 MPa).

4) The hardness distribution varied significantly between the two processes. The high hardness in rolling resulted from grain refinement and work hardening. The underwater explosive welding indicated an increase in hardness close to the interface on the Cu side. However, on the Al side, there was a tendency for hardness to decrease at the interface due to the offsetting effects of strain softening and work hardening. The formation of metal compounds in the melting layer significantly enhanced nano-hardness in both types of samples.

References

1 Elgallad E M, Samuel F H, Samuel A M, et al. *Journal of Materials Processing Technology*[J], 2010, 210(13): 1754-1766.

2 Kahveci O, Kaya M F. *International Journal of Hydrogen Energy*[J], 2022, 47(24): 12179-12188.

3 *Li J Q, Zillner J, Balle F. Materials*[J], 2023, 16(8): 3033.

4 Alexopoulos N D, Migklis V, Kourkoulis S K, et al. *Advanced Materials Research*[J], 2015, 1099: 1-8.

5 Raju P V K, Reddy M I, Harsha N, et al. *Materials Today: Proceedings*[J], 2018, 5(2): 5845-5856.

6 Ziakhor I V, Nakonechnyi A O, Qichen W, et al. *Electrometallurgy Today/Sovremennaya Elektrometallurgiya*[J], 2023 (3).

7 Jiang F, Wang W Q, Zhang X G, Gong W B. *Metals*[J], 2023, 13(12): 1969.

8 Zhou Y Y, Jiang F C, Wang Z Q, Chen J Y. *Journal of Materials Processing Technology*[J], 2023, 313: 117884.

9 Ran M T, Bian G B, Zhang H W, Yan J, Wang W X. *Journal of Manufacturing Processes*[J], 2024, 119: 224-234.

10 Dhara S, Finuf M, Zediker M, et al. *Journal of Materials Processing Technology*[J], 2023, 317: 117989.

11 Tayebi P, Nasirin A R, Akbari H, et al. *Metals*[J], 2024, 14(2): 214.

12 Athar M M H, Tolaminejad B. *Materials & design*[J], 2015, 86: 516-525.

13 Kaya Y. *Metals*[J], 2018, 8(10): 780..

14 Jandaghi M R, Saboori A, Khalaj G, et al. *Metals*[J], 2020, 10(5): 634.

15 Payak V, Paulraj J, Roy B S, et al. *Part E: Journal of Process Mechanical Engineering*[J], 2024, 238(3): 1462-1506.

16 Barekatain H, Kazeminezhad M, Kokabi A H. *Journal of Materials Science & Technology*[J], 2014, 30(8): 826-834.

17 Wang Y, Liao Y, Wu R Z, Nodir T, Chen H T, Zhang J H, et al. *Materials Science and Engineering: A*[J], 2020, 787: 139494.

18 Chang Q H, Gao P K, Zhang J Y, Huo Y Q, Zhang Z, Xie J P. *Materials*[J], 2022, 15(22): 8139.

19 Sas-Boca I M, Iluțiu-Varvara D A, Tintelecan M, et al. *Materials*[J], 2022, 15(24): 8807.

20 Wei Y N, Li H, Sun F, Zou J T. *Metals*[J], 2019, 9(2): 237.

21 Jiang L, Luo N, Liang H, Zhao Y. *The International Journal of Advanced Manufacturing Technology*[J], 2022, 123(9): 3021-3031.

22 Blazynski T Z. *Explosive welding, forming and compaction*[M]. Springer Science & Business Media, 2012.

23 Rong K. *Coal Mine Blasting*[J]. 2022,40(2):4-7.

24 Liu W, Xia Z Y, Ma L B, Wang Z F, Wang M. *Coal Mine Blasting*[J], 2020,38(3):14-18.

25 Hokamoto K, Fujita M, Shimokawa H, et al. *Journal of Materials Processing Technology*[J], 1999, 85(1-3): 175-179.

26 Zhou D P. Coal *Mine Blasting*[J], 2023,41(1):17-22.

27 Hokamoto K, Ujimoto Y, Fujita M. *Materials transactions*[J], 2004, 45(9): 2897-2901.

28 Yu Y, Ma H, Zhao K, Shen Z, Chen Y. *Central European Journal of Energetic Materials*[J], 2017, 14(1).

29 Habib M A, Keno H, Uchida R, et al. *Journal of Materials Processing Technology*[J], 2015, 217: 310-316.

30 Sun W, Li X j, Yan H H, Hokamoto K. *Journal of materials engineering and performance*[J], 2014, 23: 421-428.

31 Kou S. *Jom*[J], 2003, 55: 37-42.

32 Wang K, Kuroda M, Chen X. *Metals*[J], 2022, 12(8): 1354.

33 Chen X, Inao D, Tanaka S, Akihisa M, Li X J, Hokamoto K. *Journal of Manufacturing Processes*[J], 2020, 58: 1318-1333.

34 Li C, Li D X, Tao X M, Chen H M, Ouyang Y F. *Modelling and Simulation in Materials Science and Engineering*[J], 2014, 22(6): 065013.

35 Huang J W, Liang G F, Luo N, Li X J, Chen X, Hu J N. *Journal of Materials Research and Technology*[J], 2023, 27: 2508-2523.

36 Bataev I A, Tanaka S, Zhou Q, Lazurenko D.V., Jorge Junior A. M., Bataev A A, et al. *Materials & Design*[J], 2019, 169: 107649.

37 Yu Q, Liu X, Sun Y. *Science China Materials*[J]. 2015, 58(7): 574-583.

38 Chen D G, Zhang H M, Zhao D D, Liu Y Y, Jiang J Y. *Materials Letters*[J], 2022, 322: 132491.

39 Jiang L, Luo N, Liang H H, Zhao Y. *The International Journal of Advanced Manufacturing Technology*[J], 2022, 123(9): 3021-3031.

40 Bian X Q, Wang A Q, Xie J P, Liu P, Mao Z P, Liu Z W. *Nanotechnology*[J], 2023, 34(44): 445702.

41 Wang C, Ma X G, Ma L, Jiang Z Y, Hasan M,. Islam M A, et al. *Materials Characterization*[J], 2023, 205: 113315.

42 Martynenko N, Rybalchenko O, Bodyakova A, et al. *Materials*[J], 2022, 16(1): 105.

43 Yang X R, Zhu Z, Liu X Y, Luo L, Zhao X C. *Rare metal materials and engineering*[J], 2019, 48(3): 815-819.

44 Han S . *Phase transformation and fractography of interface of explosive welding*[M]//Beijing: National Defense Industry Press. 2011: 2-7.

45 Aghamohammadi H, Hosseinipour S J, Rabiee S M, et al. *Materials Chemistry and Physics*[J], 2021, 273: 125130.

46 Saikrishna N, Reddy G P K, Munirathinam B, et al. *Journal of magnesium and alloys*[J]. 2018, 6(1): 83-89

轧制和水下爆炸焊接制造的铜/铝复合板的界面和力学性能比较

周大鹏 [1, 2]，　刘中枢 [3, 4]，　黄佳雯 [3, 4*]，　陈金华 [1, 2*]，　陈翔 [3, 4*]，　周晓红 [1, 2]

（1. 中煤科工集团淮北爆破技术研究院有限公司，安徽 235099）

（2. 爆炸能量利用与控制安徽省重点实验室，安徽 235099）

（3. 江汉大学精细爆破国家重点实验室，武汉 430056）

（4. 江汉大学爆破工程湖北省重点实验室，武汉 430056）

摘　要：铜/铝复合材料因其轻质和优异的导电性能而被广泛应用于各行各业。然而，不同的制造方法对这些复合材料的界面结构和机械性能的影响仍然很大。在这项研究中，采用轧制和水下爆炸焊接技术制造了铜/铝复合板，系统地比较了它们的界面微观结构和机械性能。通过光学显微镜、扫描电子显微镜和电子反向散射衍射分析了界面形态、晶粒取向、晶界特征和相分布。通过拉伸剪切试验、90°弯曲试验和硬度测量评估了力学性能，其中维氏硬度和纳米压痕试验进一步揭示了硬度分布。结果表明，轧制的铜/铝复合材料中的扩散层相对较弱，而通过水下爆炸焊接产生的复合材料则具有约 18 μm 厚的扩散层，通过原子扩散形成冶金结合。这些复合材料的拉伸剪切强度介于 64.14 至 70.84 兆帕之间，水下爆炸焊接样品在 90° 三点弯曲试验中表现出更优越的弯曲性能。本研究阐明了不同制造方法对铜/铝复合材料界面性能和力学性能的影响，为选择制造方法和应用提供了重要启示。

关键词：水下爆炸焊接；铜/铝复合材料；轧制；EBSD；纳米压痕